

Reducing Curtailed Wind Energy Through Energy Storage and Demand Response

Hamideh Bitaraf¹, *Student Member, IEEE*, and Saifur Rahman, *Life Fellow, IEEE*

Abstract—Curtailed wind energy is a challenge in utilities with high wind energy penetration. This happens mainly when wind generation exceeds load minus the minimum stable operating point of generation units. At first, the role of generation mix on the curtailed wind energy is analyzed. Then, demand response (DR) applications are modeled to quantify additional reductions in the curtailed wind energy. The uniqueness of this approach is that the impact of the DR rebound effect on the system load shape can be directly reflected. This allows scheduling of DR such that the rebound period (higher demand) aligns itself with high wind output period. This minimizes the need for curtailment. Next, the issue of charging/discharging different large-scale energy storage technologies (e.g., compressed air energy storage, pumped hydro energy storage, and batteries) is addressed. This allows their impact on wind curtailment to be analyzed in detail. Finally, various combinations of energy storage and DR options are considered for investigating their impacts on further reducing wind curtailments. This problem is formulated as a mixed integer linear programming using wind and load data from Bonneville Power Administration.

Index Terms—Curtailed wind energy, demand response, energy storage, rebound effect.

I. INTRODUCTION

HIGH wind energy penetration is a potential future scenario that can result from various green energy policies. Denmark, Portugal and Spain are top three countries with the highest percentage of electricity from wind with respect to overall electricity generation [1]. There are plans for 50% or more of annual electricity generation in Denmark to come from renewables by 2020 [2].

Wind curtailment occurs due to the non-correlation between wind and load profiles during high wind electricity output periods when the load is lower. The term non-correlation used in this paper refers to the fact that wind or any other renewable generation, which is nature driven, does not follow the load like conventional power plants. In cases where wind generation is more than load minus must-run generation, the excess of wind

energy needs to be curtailed to keep the balance between demand and supply. This challenge can be mitigated by increasing flexible resources in the system, such as energy storage and demand response [3]. It is possible to partially deal with the variable and stochastic generation from renewable sources by cycling intermediate power plants, but the downside of this strategy is fatigue and increased rates of maintenance. Wind curtailment is an issue in stand-alone (island) systems with no interconnections for importing or exporting electricity which is the assumption in this paper. The economic and dynamic security issues for an island system with high wind energy penetration is discussed in [42].

The optimal DR aggregation in energy and reserve markets was fully investigated in [4]. The security-constrained unit commitment for hourly DR as load shifting and load reduction was proposed in [5], [6] for economic and security purposes. DR cost analysis with wind integration using decision tree approach has been addressed in [7]. A phenomenon associated with DR is called rebound effect that happens commonly in practice when DR ends [8]. For example, there is a rebound peak in which facilities delay their demand to avoid a peak, but cause a new peak when trying to satisfy delayed demand. Rebound effect occurs after DR ends, because control signals are synchronized to bring back loads to normal operation [9].

Energy storage sizing to minimize investment and operating costs was studied in [2]–[11]. Smoothing out the combined power output of wind farm and energy storage was investigated in [12]–[15]. The impact of energy storage to improve availability and reliability of renewable energy resources was studied in [16]–[18]. Sizing energy storage in existence of coal power plants was proposed in [19]. A variety of heuristic methods and game theory approach were used to solve energy storage sizing problem [20], [21].

Scheduling energy storage and demand response in commercial buildings has been studied in [22]. Optimal scheduling based on locational marginal price is proposed in [23]. Coordination of energy storage and DR for smoothing out the tie line power or decreasing carbon emissions was addressed in [24] and [25]. The multi-agent approach was proposed in [26] to minimize the cost and reduce peak load by managing DR and energy storage at distribution level. Simple models for scheduling of DR and energy storage were presented in [27], [28] to minimize operational costs. Authors addressed mitigating wind power forecast error by scheduling Sodium Sulfur (NaS) battery and compressed air energy storage (CAES) using signal processing techniques in [29]. Detailed modeling of NaS battery and CAES, including

Manuscript received July 8, 2016; revised November 5, 2016 and May 10, 2017; accepted June 29, 2017. Date of publication July 11, 2017; date of current version December 14, 2017. This work was supported by the National Science Foundation under Grant 11-04023, “US-Egypt Cooperative Research: Managing Grid Integration of Large-Scale Wind Power Parks Using Energy Storage Technology and Demand Response,” PI—S. Rahman. Paper no. TSTE-00517-2016. (*Corresponding author: Hamideh Bitaraf.*)

The authors are with the Advanced Research Institute, Virginia Polytechnic Institute and State University, Arlington, VA 22203 USA (e-mail: bhamideh@vt.edu; srahman@vt.edu).

Color versions of one or more of the figures in this paper are available online at <http://ieeexplore.ieee.org>.

Digital Object Identifier 10.1109/TSTE.2017.2724546

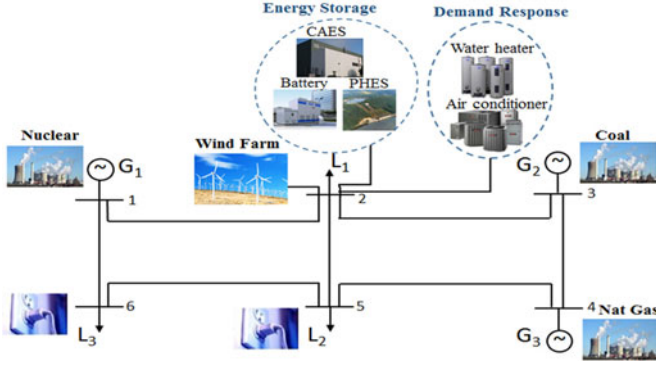


Fig. 1. Modified IEEE 6 bus system integrated with wind, energy storage, DR.

required idle time for switching between charge and discharge modes, was presented by authors in [29] to maximize wind energy penetration level.

The objective of this paper is to propose a planning tool for electric utility operators to provide an insight into the sizing and operation of grid-scale energy storage technologies and demand response programs. Contributions and novelties of this paper are summarized as follows.

In utilities with high wind energy penetration demand response needs to be implemented based on the net load profile rather than the load profile. The first contribution of this paper is controlling demand response and its rebound effect to reduce the wind curtailment. This is a not a typical demand response application such as peak load reduction. The novel idea is scheduling demand response and controlling rebound effect in such a way that its rebound effect aligns with high wind generation and low load times to reduce the curtailed wind energy. The demand response modeled in this research is based on the contract that customers allow the utility to reduce their demand for limited times and duration to get incentive payments. This idea is implemented based on a concept that the rebound effect can be controlled for a large number of consumers. This control is achievable by DR strategies proposed in [41] to return each delayed load to normal condition slowly. The frequency change is the signal which demand responds to in this research, because it varies by the mismatch between the load and the generation. The other contribution of this paper is to investigate the impact of scheduling both energy storage and DR on reducing the curtailed wind energy and comparing the effectiveness of different combinations.

The rest of the paper is organized as follows. Section II describes the system modeling. Case studies and discussions are presented in Section III.

II. SYSTEM MODELING

The whole system topology is depicted in Fig. 1 as a modified version of IEEE 6 bus system. Generation is provided by natural gas, coal, and nuclear power plants in addition to a wind farm. Different large-scale batteries, CAES and pumped hydro energy storage (PHEs) are integrated as energy storage units. Electric

water heater and air conditioner represent devices for deploying DR in Fig. 1.

The objective function is to minimize the total generation cost throughout the one-year simulation time horizon as shown in (1). The first term in (1) is related to conventional generation units as nuclear, coal, and natural gas power plants. The second term in (1) shows the cost of wind generation which excludes the curtailed wind generation. Wind generation has free fuel source but other expenses as maintenance makes this generation cost to be non-zero. Energy Storage and DR are assumed to be owned by the system operator as flexible sources; hence their associated costs did not appear in the objective function. The discussion on DR incentive schemes will be provided in the result section.

$$\text{Min} \sum_{t=1}^T \left(\left(\sum_{i=1}^G C_i p_{i,t} \Delta t \right) + C_w (p_{w,t} - p_{cw,t}) \Delta t \right) \quad (1)$$

Where,

- $p_{G,t}$: The conventional generation for nuclear, coal, and natural gas in MW
- $p_{w,t}$: The power of wind generation in MW
- $p_{cw,t}$: Curtailed wind power in MW
- C_G : Variable cost of the generation unit in \$/MWh
- C_w : Variable cost of wind generation in \$/MWh
- Δt : Duration of each time interval
- G : Number of generation units including nuclear, coal, and natural gas.
- T : Number of total time intervals

Equality and inequality constraints are defined as follows.

A. Power Balance Equation

At each interval, the total generation is equal to the demand:

$$p_{l,t} - q_{DR,t} + q_{Rb,t} = p_{w,t} + \sum_{i=1}^G p_{i,t} + p_{dchg,t} - p_{chg,t} - p_{cw,t}, \forall t \quad (2)$$

Where,

- $p_{l,t}$: Electricity load at time t in MW
- $q_{DR,t}$: DR electricity load reduction at time t in MW
- $q_{Rb,t}$: Rebound effect load increase at time t in MW
- $p_{chg,t}$: Energy storage charging power at time t in MW
- $p_{dchg,t}$: Energy storage discharging power at time t in MW

B. DR Modeling

Quantity of load reduction:

$$u_{DR,t} \tau_{DR}^{\min} p_{l,t} \leq q_{DR,t} \leq u_{DR,t} \tau_{DR}^{\max} p_{l,t}, \forall t \quad (3)$$

Where,

- $u_{DR,t}$: Binary variable denoting if load is reduced at time t; 1 if demand is reduced, 0 otherwise
- τ_{DR}^{\max} : Maximum DR quantity limit ratio over load
- τ_{DR}^{\min} : Minimum DR quantity limit ratio over load

Ramping rate limit of DR:

$$\begin{aligned} -r_{DR}\tau_{DR}^{\max}p_{l,t} &\leq (q_{DR,t} - q_{DR,t-1})/\Delta t \\ &\leq r_{DR}\tau_{DR}^{\max}p_{l,t}, t > 1 \end{aligned} \quad (4)$$

Where,

r_{DR} : DR Ramp rate limit ratio over DR

A constraint for minimum duration of load reduction:

$$\sum_{t'=t}^{t+T_{DR}^{\min}-1} u_{DR,t'} \geq T_{DR}^{\min} y_{DR,t}, \forall t \quad (5)$$

Where,

$y_{DR,t}$: The binary starting indicator of DR

T_{DR}^{\min} : Minimum duration of DR in hrs.

A constraint for maximum duration of load reduction:

$$\sum_{t'=t}^{t+T_{DR}^{\max}-1} z_{DR,t'} \geq y_{DR,t}, \forall t \quad (6)$$

Where,

$z_{DR,t}$: The binary stopping indicator of DR

T_{DR}^{\max} : Maximum duration of DR in hrs.

A constraint for minimum duration of idle state from last DR event:

$$\sum_{t'=t}^{t+T_{DR,idle}^{\min}-1} (1 - u_{DR,t'}) \geq T_{DR,idle}^{\min} z_{DR,t}, \forall t \quad (7)$$

Where,

$T_{DR,idle}^{\min}$: Minimum time of 'idle state' from last DR

Rebound effect is another restrike after DR which occurs when all delayed loads come back to operation at the same time. The presented modeling in this paper is based on the concept that delayed loads can be controlled to come back to normal operation by aggregators. Hence, the rebound effect is controllable by duration, ramp rate, and energy ratio constraints in (8), (9), and (10), respectively to be integrated in the economic dispatch problem.

A constraint for rebound effect duration from last DR:

$$u_{Rb,t}\tau_{Rb}^{\min}p_{l,t} \leq q_{Rb,t} \leq \tau_{Rb}^{\max}p_{l,t} \sum_{t'=1}^{T_{Rb}} z_{DR,t-t'+1}, \forall t \quad (8)$$

Where,

$u_{Rb,t}$: The binary rebound effect status at time t; 1 if occurred, 0 otherwise

τ_{Rb}^{\min} : Min rebound effect limit ratio over load in %

τ_{Rb}^{\max} : Maximum rebound effect ratio over load in %

T_{Rb} : Duration of rebound effect profile in hrs.

Ramp rate limit of rebound effect:

$$-r_{Rb}\tau_{Rb}^{\max}p_{l,t} \leq (q_{Rb,t} - q_{Rb,t-1})/\Delta t \leq r_{Rb}\tau_{Rb}^{\max}p_{l,t}, t > 1 \quad (9)$$

Where,

r_{Rb} : Rebound effect Ramp rate limit ratio in %

The energy ratio between rebound effect and last DR is formulated as follows.

$$\sum_{t=1}^{Daily} q_{Rb,t} = \lambda \sum_{t=1}^{Daily} q_{DR,t} \quad (10)$$

Where,

λ : Ratio of rebound effect energy to DR energy

Maximum number of weekly DR events:

$$\sum_{t=1}^T y_t \leq N_{Weekly} \quad (11)$$

Where,

N_{Weekly} : Maximum number of weekly DR events

Maximum number of daily DR events:

$$\sum_{t=1}^{Daily} y_t \leq N_{Daily} \quad (12)$$

Where,

N_{Daily} : Maximum number of Daily DR events

Relationships among binary variables associated with DR:

$$y_{DR,t} - z_{DR,t} = u_{DR,t} - u_{DR,t-1}, \forall t \quad (13)$$

$$y_{DR,t} + z_{DR,t} \leq 1, \forall t \quad (14)$$

The relationship among binary variables of DR and rebound effect stating that rebound effect starts right after DR ends

$$\sum_{t=1}^{t'} z_{DR,t} = u_{Rb,t'}, t' = T_{Rb} : T \quad (15)$$

C. Large-Scale Mechanical Energy Storage

This part models detailed characteristic of mechanical energy storage units including PHES and CAES, as follows.

Final state of charge (SoC) equals to initial SoC weekly.

$$\sum_{t'}^{weekly} (p_{chg,t'}\eta_{ES} - p_{dchg,t'})\Delta t = 0 \quad (16)$$

Where,

η_{ES} : Roundtrip efficiency of energy storage in %

Mechanical energy storage can operate at one mode only: charge, discharge, or idle.

$$\alpha_{ES,t} + \beta_{ES,t} + \gamma_{ES,t} = 1, \forall t \quad (17)$$

Where,

$\alpha_{ES,t}$: The binary charging status of energy storage at time t; 1 if charging, 0 otherwise

$\beta_{ES,t}$: The binary discharging status of energy storage at time t; 1 if discharging, 0 otherwise

$\gamma_{ES,t}$: Binary idle status of energy storage at time t; 1 if idle, 0 otherwise

Relationships among start and stop indicators of idle time:

$$\rho_{ES,t} - \phi_{ES,t} = \gamma_{ES,t} - \gamma_{ES,t-1}, t > 1 \quad (18)$$

$$\rho_{ES,t} + \phi_{ES,t} \leq 1, \forall t \quad (19)$$

Where,

$\rho_{ES,t}$: Binary starting indicator of idle mode at time t

$\phi_{ES,t}$: Binary stopping indicator of idle mode at time t ,

Relationships among binary variables indicating that if the mode of operation changes it should remain idle:

$$\rho_{ES,t} - \phi_{ES,t} = \alpha_{ES,t-1} - \alpha_{ES,t} + \beta_{ES,t-1} - \beta_{ES,t}, t > 1 \quad (20)$$

$$-1 \leq (\alpha_{ES,t-1} - \alpha_{ES,t}) + (\beta_{ES,t-1} - \beta_{ES,t}) \leq 1, t > 1 \quad (21)$$

Charging/discharging power limited constraint:

$$P_{ES} N_{ES} \alpha_{ES,t} \mu_{ES,chg}^{\min} \leq p_{chg,t} \leq P_{ES} N_{ES} \alpha_{ES,t}, \forall t \quad (22)$$

$$P_{ES} N_{ES} \beta_{ES,t} \mu_{ES,dchg}^{\min} \leq p_{dchg,t} \leq P_{ES} N_{ES} \beta_{ES,t}, \forall t \quad (23)$$

Where,

P_{ES} : Rated power of energy storage in MW

N_{ES} : Number of energy storage units

$\mu_{ES,chg}^{\min}$: Minimum energy storage charging power operational limit in %

$\mu_{ES,dchg}^{\min}$: Minimum energy storage discharging power operational limit in %

The minimum required idle time to switch between modes:

$$\sum_{t'=t}^{t+T_{ES}^{\min}-1} \gamma_{ES,t'} \geq T_{ES}^{\min} \rho_{ES,t}, \forall t \quad (24)$$

Where,

T_{ES}^{\min} : Minimum storage idle mode duration in hrs.

State of charge is limited to rated energy capacity:

$$0 \leq \frac{\sum_{t'=1}^k (p_{chg,t'} \eta_{ES} - p_{dchg,t'}) \Delta t}{E_{ES} N_{ES}} + SOC_{ES}^{\text{int}} \leq 1, k = 1 : T \quad (25)$$

Where,

E_{ES} : Energy capacity of energy storage in MWh

SOC_{ES}^{int} : Initial state of charge of energy storage

Ramp rate constraint of energy storage:

$$\begin{aligned} -r_{ES} N_{ES} &\leq \frac{(p_{chg,t} - p_{dchg,t}) - (p_{chg,t-1} - p_{dchg,t-1})}{\Delta t} \\ &\leq r_{ES} N_{ES}, t > 1 \end{aligned} \quad (26)$$

Where,

r_{ES} : Energy storage ramp rate in MW/15 min

D. Large-Scale Battery

The batteries are daily refilled. Hence, the final state of the charge equals to the initial state of charge every day.

$$\sum_{t'}^{\text{Daily}} (p_{chg,t'} \eta_{ES} - p_{dchg,t'}) \Delta t = 0 \quad (27)$$

Charging and discharging powers are limited to rated power capacity of energy storage:

$$0 \leq p_{chg,t}, p_{dchg,t} \leq P_{ES} N_{ES}, \forall t \quad (28)$$

State of the charge is limited to maximum and minimum allowable state of charge considering rated energy capacity:

$$SOC_{ES,t} = \frac{\sum_{t'=1}^t (p_{chg,t'} \eta_{ES} - p_{dchg,t'}) \Delta t}{E_{ES} N_{ES}} + SOC_{ES}^{\text{int}} \quad (29)$$

$$SOC_{ES}^{\min} \leq SOC_{ES,t} \leq SOC_{ES}^{\max}, t = 1 : T \quad (30)$$

Where,

$SOC_{ES,t}$: Energy storage state of charge at time t in %

SOC_{ES}^{\min} : Minimum state of charge in %

SOC_{ES}^{\max} : Maximum state of charge in %

E. Equivalent Natural Gas and Coal Unit Modeling

(The term equivalent means in this paper that all of those units are treated as a group.)

Power limit:

$$P_G \mu_G^{\min} u_{G,t} \leq p_{G,t} \leq P_G u_{G,t}, \forall t \quad (31)$$

Where,

$u_{G,t}$: Binary variable denoting generation unit is on or off at time t ; 1 if on, 0 otherwise

P_G : Power capacity of the generation unit in MW

μ_G^{\min} : Minimum stable generation of units in %

Relationships among binary variables:

$$y_{G,t} - z_{G,t} = u_{G,t} - u_{G,t-1}, t > 1 \quad (32)$$

$$y_{G,t} + z_{G,t} \leq 1, \forall t \quad (33)$$

Where,

$y_{G,t}$: Binary starting indicator of generation unit

$z_{G,t}$: Binary stopping indicator of generation unit

Ramp rate limit:

$$-r_G \leq (p_{G,t} - p_{G,t-1}) / \Delta t \leq r_G, \forall t \quad (34)$$

Where,

r_G : Ramp rate of conventional generation unit in MW/min

Minimum up time constraint:

$$\sum_{t'=t}^{t+T_{G,up}^{\min}-1} u_{G,t'} \geq T_{G,up}^{\min} y_{G,t}, \forall t \quad (35)$$

Where,

$T_{G,up}^{\min}$: Minimum up time of generation unit in hrs.

Minimum down time constraint:

$$\sum_{t'=t}^{t+T_{G,dn}^{\min}-1} (1 - u_{G,t'}) \geq T_{G,dn}^{\min} z_{G,t}, \forall t \quad (36)$$

Where,

$T_{G,dn}^{\min}$: Minimum down time of the unit in hrs.

Capacity factor constraint: this is only applied to Coal unit to guarantee its economic operation, while natural gas unit is considered as peaking unit and do not have this constraint.

$$CF_G^{\min} \leq \sum_{t=1}^T p_{G,t} \leq CF_G^{\max} \quad (37)$$

Where,

CF_G^{\min} : Minimum capacity factor limit in %

CF_G^{\max} : Maximum capacity factor limit in %

F. Equivalent Nuclear Unit Modeling

Power limit:

$$P_G \mu_G^{\min} \leq p_{G,t} \leq P_G, \forall t \quad (38)$$

Ramp rate limit:

$$-r_G \leq (p_{G,t} - p_{G,t-1})/\Delta t \leq r_G, \forall t \quad (39)$$

Capacity factor constraint:

$$CF_G^{\min} \leq \sum_{t=1}^T p_{G,t} \leq CF_G^{\max} \quad (40)$$

G. Network Modeling

The power flow in each line is limited to the thermal limit of that line as shown in 41 and is derived by DC power flow.

$$-P_{line}^{\max} \leq p_{line,t} \leq P_{line}^{\max}, \forall t \quad (41)$$

Where,

$p_{line,t}$: Power flow through the lines at time t in MW

P_{line}^{\max} : Maximum thermal limit of the line in MW

III. CASE STUDIES AND DISCUSSIONS

To showcase the applicability of the proposed approach, different case studies based on real world wind and load data with 15-minute interval, obtained from the Bonneville Power Administration (BPA) for the whole year of 2013, are used [31]. BPA peak load in 2013 was 10.6 GW, and installed wind capacity was 4.5 GW [31]. BPA load is scaled up to meet projected load in 2040 using average rate growth of 0.8% per year from 2013 to 2040 [32]. Wind data is also scaled up to reach the 20% annual wind energy penetration level. The mixed integer linear programming (MILP) is modeled in MATLAB and solved by IBM CPLEX with the time horizon of one year with 15-minute time resolution. Since the optimization constraints are defined independent for each week, the optimization problem is simulated for fifty-two weeks separately and results are the summation of all.

Parameters for modeling generation units by fuel type are presented in Table I. As shown, nuclear power plants can ramp down by 20% of nominal capacity per hour, but ramping up the same amount takes 6 to 8 hours [33]. Minimum stable operation of nuclear generation is 80% of nominal capacity, while minimum operation of Natural Gas unit is 20% of its rated capacity. If availability is 90% for each generation units, then installed capacity is required to be 11% more to be able to provide desired generation throughout the year. The maintenance and forced outage rates of conventional power plants have been neglected in this study. The cost of energy for each type of generation is shown in Table I as well based on forecasted Levelized Cost of Energy reported by US EIA for 2040 [43].

Modeling parameters for mechanical energy storage units including CAES and PHES are presented in Table II. PHES

TABLE I
PARAMETERS OF GENERATION UNITS [33], [43]

Unit Type by Fuel	Nat Gas	Coal	Nuclear	Wind
Min Stable Generation (%)	20	30	80	—
Ramp Up/Down	8% per min	1.5% per min	20% per hr down, 20% per 6 hrs up	—
Min Up/Down Time	2 hrs	12 hrs	—	—
Capacity Factor (%)	—	45–70	75–100	—
LCOE (\$/MWh)	108.1	125.8	93	58.8

TABLE II
LARGE-SCALE MECHANICAL ENERGY STORAGE PARAMETERS [37]–[39]

Energy Storage Technology	PHES		
	Single Speed	Adjustable Speed	CAES
Generating Range (%)	100-50	100-30	100-0
Pumping Range (%)	100-100	100-40	100-0
Power Capacity (MW)	300	—	300, 600
Energy Capacity (MWh)	6000	—	6000
Ramp Rate	4–6% /second	—	18 MW/min
Efficiency (%)	80	—	70
Required Idle Time to Switch Modes (min)	4	—	20

TABLE III
LARGE-SCALE BATTERIES PARAMETERS [38], [39]

Grid-scale battery	Power (MW)	Energy (MWh)	Efficiency (%)	Max, Min SoC
NaS	50	300	75	0.9, 0.1
Lead acid	50	200	85	0.9, 0.1

technologies are either fixed speed or adjustable speed. Fixed speed PHES can only pump at constant power, while adjustable speed one pumps for a specific range. The rated energy and power capacities for both CAES and PHES are considered to be 6000 MWh and 300 MW, respectively, for better comparison between these two technologies. CAES has another scenario for power capacity which is 600 MW. Characteristics of large-scale batteries including NaS, Lead acid are shown in Table III.

DR amount can be estimated by aggregated amount of electric water heater and air conditioning, participation factor, and capacity response ratio [34]. Total amount of DR in U.S. is 9.2% of the peak load in 2012 [35]. This paper assumes 5% and 10% of load at that time for DR maximum amount as shown in Table IV. DR ramp rate in 15 minutes is assumed to be half of DR value at that time, due to 30-minute DR response time and 15-minute time resolution of the study [36]. As shown the rebound effect to load reduction energy ratio is one. This address delaying the load consumption such as a washer dryer, that the rebound effect energy is the same as the load reduction energy. Hence, the total energy of load consumption before and after DR remains the same.

TABLE IV
DR AND REBOUND EFFECT MODELING PARAMETERS

	Max	Min
Load Reduction Power to Load Ratio	0.05, 0.10	0.01
Duration of DR (hrs)	3	2
Rebound Effect Power to Load Ratio	0.05, 0.10	0.01
Ramp Rate of DR to Max Load Reduction Ratio	0.5	
Min Duration of Idle Time from Last DR (hrs)	3	
Duration of Rebound Effect (hrs)	2	
Ramp Rate of Rebound Effect to Max Load Reduction Ratio	0.5	
Rebound Effect to Load Reduction Energy Ratio	1	
Max Number of DR Events in a Week	3	
Max Number of DR Events in a Day	1	

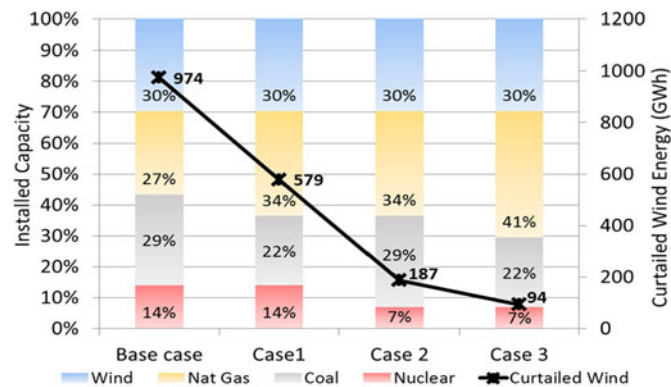


Fig. 2. Different generation mix and their resultant wind curtailment.

For example, if rebound to DR energy ratio is 0.5, then, DR reducing 1000 MWh of load has a rebound with 500 MWh energy. Other characteristics of DR, like maximum three events per week and one event daily are shown in Table IV.

Different case studies are simulated to study the impact of generation mix, different DR scenarios, different energy storage technologies, and scheduling both DR and energy storage on reducing the curtailed wind energy. These case studies and their results are described as follows.

A. Impact of Generation Mix by Fuel Type

Four different generation mix scenarios including the projected generation in 2040 by U.S. EIA [32] are used to study their impacts on the curtailed wind energy. As shown in Fig. 2, the installed wind capacity is the same for each case.

As shown in Fig. 2, the base case results in 974 GWh curtailed wind energy. This curtailment is 7% of the annual wind energy generation. The base case has the highest curtailed wind energy due to having the highest nuclear and coal capacity comparing to the other cases. Then, case 1 with 10% less coal generation and 10% more gas generation units while having the same capacity comparing to the base case, results in 579 GWh curtailed wind energy. Hence, the curtailed wind energy has reduced by 395 GWh for case 1 as compared to the base case. The nuclear capacity has reduced by 10% and gas has increased by 10% for case 2 as compared to base case. This generation mix of case 2 results in 787 GWh less curtailed wind energy as compared to

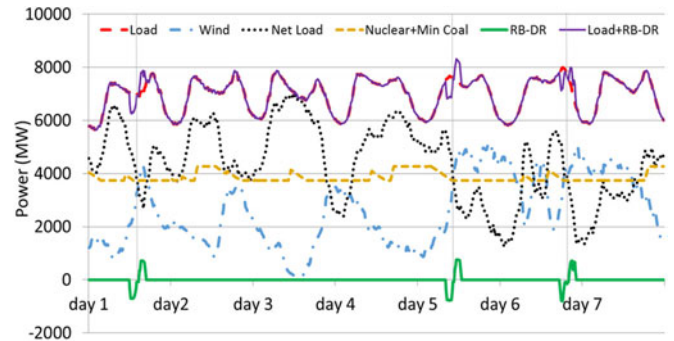


Fig. 3. Load, wind, and 10% DR followed by rebound effect for a week.

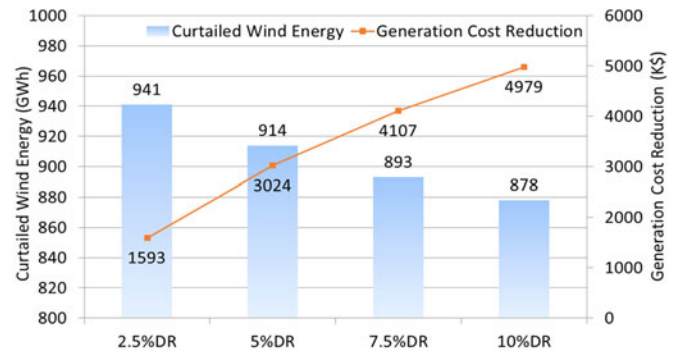


Fig. 4. Curtailed wind energy for different DR scenarios.

base case. The curtailed wind energy of case 3 is the least which is 94 GWh due to having the lowest nuclear and coal generation capacity. The results shown in Fig. 2 vary for each case due to different flexibility that each generation unit provides for balancing services. Hence, generation units with more flexibility can cope up with variable generation of wind and result in less curtailed wind energy. This conclusion is due to the flexibility not the fuel type. The generation mix for the rest of case studies is based on the base case study.

B. Impact of Different DR Scenarios

The novel idea presented is controlling DR and rebound effect such that it can reduce curtailed wind energy. The sample result of the optimization problem for a week is shown in Fig. 3. DR is scheduled prior to high wind energy penetration periods such that its rebound effect is aligned with the time of high wind generation period. This unique DR scheduling can reduce curtailed wind energy by adjusting the rebound effect occurring time. The negative part of the green line shown in Fig. 3 is DR (load reduction) and the positive one is related to the rebound effect (load compensation). The load profile after DR is depicted in Fig. 3 as a purple line.

The impact of different DR scenarios on curtailed wind energy is shown in Fig. 4. As shown, 2.5% results in 33 GWh reductions in curtailed wind energy compared to the base case without DR implementation. 5% DR reduces curtailed wind energy by 60 GWh. As shown in Fig. 4, curtailed wind energy is reduced by 81 GWh, 96 GWh, for 7.5%, and 10% DR scenarios. Generation cost reduction by implementing different DR scenarios is shown

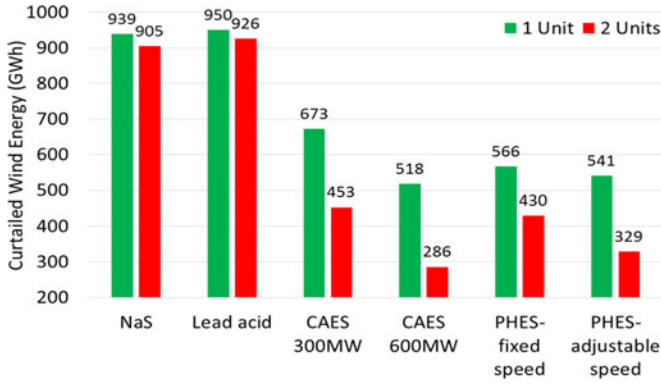


Fig. 5. Curtailed wind energy for different energy storage technologies.

in Fig. 4 by the red line. This is shown to give an insight that DR incentive schemes need to be designed to be less than this amount to keep its benefits outweighs the implementation costs. For example, 5% DR incentive schemes cost needs to be less than 3.024 M\$ for the year to keep this alternative cost efficient.

C. Impact of Different Energy Storage Technologies

The impact of large-scale energy storage technologies on curtailed wind energy reduction are shown in Fig. 5. Large-scale mechanical energy storage technologies have higher rated energy and power capacities than batteries. Hence, mechanical energy storage technologies results in less curtailed wind energy as compared to batteries. The curtailed wind energy without inserting any type of energy storage technology is 974 GWh. If one NaS battery is inserted, curtailed wind energy reaches 939 GWh. Curtailed wind energy reaches 905 GWh when one Lead acid battery is inserted, due to its lower energy capacity.

If one 300 MW CAES is inserted, curtailed wind energy reaches 673 GWh. While, scheduling two 300 MW CAES units results in 453 GWh of curtailed wind energy. The reason why curtailed wind energy reduction is not doubled by adding an additional CAES is because the remaining available curtailed wind energy is less than what was available to charge the first CAES. This is important to take into consideration for investing on adding more energy storage units. When one 600 MW CAES is inserted with the same rated energy capacity as the 300 MW CAES, then curtailed wind energy reaches 518 GWh. Hence, only doubling the rated power capacity reduces 155 GWh more of curtailed wind energy.

Variable speed PHES results in 101 GWh less curtailed wind energy as compared to fixed speed one as shown in Fig. 5. This is due to fixed pumping power of fixed speed PHES and lower range of generating power as compared to adjustable PHES. Although 600 MW CAES and both PHES technologies have the same rated power and energy capacity values, the curtailed wind energy is reduced more by CAES as compared to PHES. This is because CAES has larger range of pumping and generating powers as compared to PHES.

The results shown in Fig. 5 are based on a daily refill for batteries while mechanical energy storage technologies are operated based on a weekly basis as described. If batteries are

TABLE V
CURTAILED WIND ENERGY REDUCTION (GWH)

Battery	1 NaS	2 NaS	1 Lead acid	2 Lead acid
Daily Basis	939	905	950	926
Weekly Basis	936	899	947	922

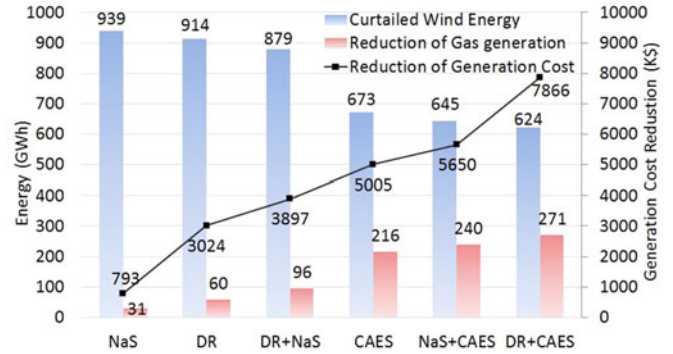


Fig. 6. Curtailed wind energy for different DR and energy storage scenarios.

operated based on weekly refill constraint, they will result in less curtailed wind energy due to more flexibility. For example, operating one NaS battery based on weekly basis results in 936 GWh of curtailed wind energy as compared to daily basis which was 939 GWh. This analysis for both NaS and Lead acid batteries are shown in Table V for a year.

D. Impact of Scheduling Both DR and Energy Storage

The impact of scheduling both energy storage and DR on reducing curtailed wind energy is depicted in Fig. 6. The 5% DR amount with rebound effect is considered for this case study. Two types of energy storage units – CAES, as a mechanical energy storage technology, and NaS battery, as a chemical energy storage technology – are selected. These two technologies are selected because they can provide less wind curtailment, as compared to their own category.

As shown, if NaS battery is inserted curtailed wind energy reaches 939 GWh. The impact of DR is seen in the following way. After DR deployment, the curtailed wind energy decreases by 60 GWh. If both DR and NaS battery are scheduled, curtailed wind energy reaches 879 GWh. If one CAES is inserted, curtailed wind energy reaches 673 GWh. By inserting one CAES, and one NaS battery, curtailed wind energy reaches 645 GWh. Scheduling one CAES and DR, reduces curtailed wind energy to 624 GWh. This better overall result in less curtailed wind energy is achieved with 10% DR.

To evaluate the cost-benefit analysis of each alternative, the generation cost reduction for each scenario is shown in Fig. 6. As shown, the cost reduction by DR and NaS scenario is 7.866 M\$ which is more than the NaS and CAES option. This analysis shows that the cost of implementing each scenario needs to be less than the resultant generation cost reduction to make the alternative cost efficient. As shown in Fig. 6, the benefit of

reducing curtailed wind energy yields to the decrease in gas generation and less carbon emission.

IV. CONCLUSION

The amount of curtailed wind energy depends on generation mix, system load, energy storage and an active demand response program. The surplus unused energy is a significant challenge in utilities with no interconnection to import/export electricity. The generation mix considered for this research includes nuclear, coal, and natural gas while each provides different flexibility for balancing services. Based on this study, decreasing nuclear capacity by 50% and increasing gas generation capacity by 20%, result in 85% reduction in the curtailed wind energy.

In high wind energy penetration cases, the peak demand depends on wind and load profiles. This paper proposes an approach to implement DR in a way that the rebound effect coincides with high wind generation and low load. The amount of this reduction depends on rebound effect and demand response parameters limited by the contract between a grid operator and energy customers. This study shows that a 10% DR reduces the curtailed wind energy by 11%.

Energy storage technologies with higher energy capacity, like CAES, can absorb more energy, which results in less curtailed wind energy. Deployment of one CAES unit results in 30% reduction in curtailed wind energy while inserting one NaS battery yields a 4% reduction in the curtailed wind energy. Scheduling CAES and DR together results in 40% reduction in curtailed wind energy, while deploying CAES and NaS battery results in 34% curtailed energy reduction.

Using Energy Storage and DR provide an opportunity to a more sustainable power system by decreasing the curtailed wind energy. The overall decision depends on comparing the cost reduction of total generation with the implementation cost of energy storage and demand response alternatives.

ACKNOWLEDGMENT

The authors would like to thank Haiwang Zhong for his assistance in the initial steps of DR modeling.

REFERENCES

- [1] L. Fried, S. Sawyer, S. Shukla, and L. Qiao, "Global wind report: Annual market update 2013," GWEC, Brussels, Belgium. [Online]. Available: gwec.net/wp-content/uploads/2014/04/GWEC-Global-Wind-Report_9-April-2014.pdf.
- [2] P. Meibom, K. B. Hilger, H. Madsen, and D. Vinther, "Energy comes together in Denmark: The key to a future fossil-free Danish power system," *IEEE Power Energy Mag.*, vol. 11, no. 5, pp. 46–55, Sep./Oct. 2013.
- [3] J. Devlin, K. Li, P. Higgins, and A. Foley, "System flexibility provision using short term grid scale storage," *IET Gener., Transm. Distrib.*, vol. 10, no. 3, pp. 697–703, Feb. 2016.
- [4] W. Hongyu, M. Shahidehpour, A. Alabdulwahab, and A. Abusorrah, "Demand response exchange in the stochastic day-ahead scheduling with variable renewable generation," *IEEE Trans. Sustain. Energy*, vol. 6, no. 2, pp. 516–525, Apr. 2015.
- [5] K. Dietrich, J. M. Latorre, L. Olmos, and A. Ramos, "Demand response in an isolated system with high wind integration," *IEEE Trans. Power Syst.*, vol. 27, no. 1, pp. 20–29, Feb. 2012.
- [6] A. Khodaie, M. Shahidehpour, and S. Bahramirad, "SCUC with hourly demand response considering intertemporal load characteristics," *IEEE Trans. Smart Grid*, vol. 2, no. 3, pp. 564–571, Sep. 2011.
- [7] S. H. Madaeni and R. Sioshansi, "Using demand response to improve the emission benefits of wind," *IEEE Trans. Power Syst.*, vol. 28, no. 2, pp. 1385–1394, May 2013.
- [8] W. Zhang, K. Kalsi, J. Fuller, M. Elizondo, and D. Chassin, "Aggregate model for heterogeneous thermostatically controlled loads with demand response," in *Proc. IEEE Power Energy Soc. Gen. Meeting*, San Diego, CA, USA, Jul. 2012, pp. 1–8.
- [9] T. Ericson, "Direct load control of residential water heaters," *Energy Policy*, vol. 37, no. 9, pp. 3502–3512, Sep. 2009.
- [10] H. T. Le, S. Santoso, and T. Q. Nguyen, "Augmenting wind power penetration and grid voltage stability limits using ESS: Application design, sizing, and a case Study," *IEEE Trans. Power Syst.*, vol. 27, no. 1, pp. 161–171, Feb. 2012.
- [11] C. Abbey and G. Joos, "A stochastic optimization approach to rating of energy storage systems in wind-diesel isolated grids," *IEEE Trans. Power Syst.*, vol. 24, no. 1, pp. 418–426, Feb. 2009.
- [12] S. Teleke, M. E. Baran, S. Bhattacharya, and A. Q. Huang, "Rule-based control of battery energy storage for dispatching intermittent renewable sources," *IEEE Trans. Sustain. Energy*, vol. 1, no. 3, pp. 117–124, Oct. 2010.
- [13] L. Xu, X. Ruan, C. Mao, B. Zhang, and Y. Luo, "An improved optimal sizing method for wind-solar-battery hybrid power system," *IEEE Trans. Sustain. Energy*, vol. 4, no. 3, pp. 774–785, Jul. 2013.
- [14] T. K. A. Brekken, A. Yokochi, A. V. Jouanne, Z. Z. Yen, H. M. Hapke, and D. A. Halamay, "Optimal energy storage sizing and control for wind power applications," *IEEE Trans. Sustain. Energy*, vol. 2, no. 1, pp. 69–77, Jan. 2011.
- [15] S. Teleke, M. E. Baran, A. Q. Huang, S. Bhattacharya, and L. Anderson, "Control strategies for battery energy storage for wind farm dispatching," *IEEE Trans. Energy Convers.*, vol. 24, no. 3, pp. 725–732, Sep. 2009.
- [16] Y. Levron, J. M. Guerrero, and Y. Beck, "Optimal power flow in micro grids with energy storage," *IEEE Trans. Power Syst.*, vol. 28, no. 3, pp. 3226–3234, Apr. 2013.
- [17] D. Gayme and U. Topcu, "Optimal power flow with large-scale storage integration," *IEEE Trans. Power Syst.*, vol. 28, no. 2, pp. 709–717, May 2013.
- [18] P. Wang, Z. Gao, and L. Bertling, "Operational adequacy studies of power systems with wind farms and energy storages," *IEEE Trans. Power Syst.*, vol. 27, no. 4, pp. 2377–2384, Nov. 2012.
- [19] C. Wang, Z. Lu, and Y. Qiao, "A consideration of the wind power benefits in day-ahead scheduling of wind-coal intensive power systems," *IEEE Trans. Power Syst.*, vol. 28, no. 1, pp. 236–245, Feb. 2013.
- [20] S. Teleke, M. E. Baran, S. Bhattacharya, and A. Q. Huang, "Rule-based control of battery energy storage for dispatching intermittent renewable sources," *IEEE Trans. Sustain. Energy*, vol. 1, no. 3, pp. 117–124, Oct. 2010.
- [21] Sh. Mei, D. Zhang, Y. Wang, F. Liu, and W. Wei, "Robust optimization of static reserve planning with large-scale integration of wind power: A game theoretic approach," *IEEE Trans. Sustain. Energy*, vol. 5, no. 2, pp. 535–545, Apr. 2014.
- [22] Z. Wang and Y. He, "Two-stage optimal demand response with battery energy storage systems," *IET Gener., Transm. Distrib.*, vol. 10, no. 5, pp. 1286–1293, Apr. 2016.
- [23] X. Fang, F. Li, Y. Wei, and H. Cui, "Strategic scheduling of energy storage for load serving entities in locational marginal pricing market," *IET Gener., Transm. Distrib.*, vol. 10, no. 5, pp. 1258–1267, Apr. 2016.
- [24] D. Wang *et al.*, "A demand response and battery storage coordination algorithm for providing microgrid tie-line smoothing services," *IEEE Trans. Sustain. Energy*, vol. 5, no. 2, pp. 476–486, Apr. 2014.
- [25] D. Pudjianto, M. Aunedi, P. Djapic, and G. Strbac, "Whole-systems assessment of the value of energy storage in low-carbon electricity systems," *IEEE Trans. Smart Grid*, vol. 5, no. 2, pp. 1098–1109, Mar. 2014.
- [26] H. S. V. S. Kumar Nunna, S. Doolla, L. Ning Lu, and K. Xiangyu, "Energy management in microgrids using demand response and distributed storage—A multi agent approach," *IEEE Trans. Power Del.*, vol. 28, no. 2, pp. 939–947, Apr. 2013.
- [27] W. Alharbi and K. Bhattacharya, "Demand response and energy storage in MV islanded microgrids for high penetration of renewables," in *Proc. IEEE Electr. Power Energy Conf.*, Halifax, NS, Canada, Aug. 2013, pp. 1–6.
- [28] K. Mackey, R. McCann, K. Rahman, and R. Winkelmann, "Evaluation of a battery energy storage system for coordination of demand response and renewable energy resources," in *Proc. 4th IEEE Int. Symp. Power Electron. Distrib. Gener. Syst.*, Rogers, AR, USA, Jul. 2013, pp. 1–8.

- [29] H. Bitaraf, S. Rahman, and M. Pipattanasomporn, "Sizing energy storage to mitigate wind power forecast error impacts by signal processing techniques," *IEEE Trans. Sustain. Energy*, vol. 6, no. 4, pp. 1457–1465, Oct. 2015.
- [30] H. Bitaraf, H. Zhong, and S. Rahman, "Managing large scale energy storage units to mitigate high wind penetration challenges," in *Proc. IEEE Power Energy Soc. Gen. Meeting*, Denver, CO, USA, Jul. 2015, pp. 1–5.
- [31] Historical BPA wind and load data 2013. [Online]. Available: transmission.bpa.gov/Business/operations/Wind/default.aspx.
- [32] J. J. Conti, P. D. Holtberg, and J. R. Diefenderfer, "Annual energy outlook 2015, with projections to 2040," U.S. Energy Inf. Admin. Office Integr. Int. Energy Anal., U.S. Dept. Energy, Washington, DC, USA. [Online]. Available: [eia.gov/forecasts/aeo/pdf/0383\(2015\).pdf](http://eia.gov/forecasts/aeo/pdf/0383(2015).pdf).
- [33] I. Perez-Arriaga, "Managing large scale penetration of intermittent renewables," in *Proc. MITEI Symp. Manag. Large-Scale Penetration Intermittent Renew.*, Cambridge, MA, USA, Apr. 2011, 43 p.
- [34] J. E. Runnels and M. D. Whyte, "Evaluation of demand side management alternatives," *Proc. IEEE*, vol. 73, no. 10, pp. 1489–1495, Oct. 1985.
- [35] M. Lee *et al.*, "Assessment of demand response and advanced metering," Fed. Energy Regul. Comm., Washington, DC, USA, Tech. Rep., 2013, 130 p.
- [36] D. K. Critz, "Power system balancing with high renewable penetration: The potential of demand response," M.S. thesis, , Eng. Syst. Div., Massachusetts Inst. Technol., Cambridge, MA, USA, 2011.
- [37] S. J. Hayes, "Technical analysis of pumped storage and integration with wind power in the Pacific Northwest," Hydroelectric Design Center, Final Rep., Aug. 2009, 166 p.
- [38] F. S. Barnes and J. G. Levine, *Large Scale Energy Storage Handbook*. Boca Raton, FL, USA: CRC Press, Mar. 2011.
- [39] R. Carnegie, D. Gotham, D. Nderitu, and P. V. Preckel, *Utility Scale Energy Storage Systems, Benefits, Application, and Technologies*. West Lafayette, IN, USA: State Utility Forecasting Group, Jun. 2013.
- [40] F. Milano, "Documentation for PSAT," Feb. 2008.
- [41] N. Motegi, M. A. Piette, D. S. Watson, S. Kiliccote, and P. Xu, "Introduction to commercial building control strategies and techniques for demand response," Lawrence Berkeley Nat. Lab., Berkeley, CA, USA, LBNL-59975, 2007.
- [42] N. Hatziargyriou *et al.*, "Security and economic impacts of high wind power penetration in island systems," in *Proc. 2004 CIGRE Conf.*, Paris, 2004, pp. 1–9.
- [43] "Levelized cost and levelized avoided cost of new generation resources in the annual energy outlook 2016," U.S. Energy Inf. Admin., Washington, DC, USA, Aug. 2016.

Hamideh Bitaraf (S'11) received the B.S. and M.S. degrees from the Electrical Engineering Department, Sharif University of Technology, Tehran, Iran, in 2010 and 2012, respectively. She is currently working toward the Ph.D. degree in the Bradley Department of Electrical and Computer Engineering, Virginia Polytechnic and State University, Blacksburg, VA, USA. She has been a Graduate Research Assistant with Virginia Tech – Advanced Research Institute, Arlington, VA, USA, since 2012. Her research interests include energy storage, wind power, demand response, renewable energy, and smart grid, signal processing, and optimization methods.

Saifur Rahman (S'75–M'78–SM'83–F'98–LF'16) is the Founding Director of the Advanced Research Institute at Virginia Tech, Arlington, VA, USA, where he is the Joseph R. Loring Professor of electrical and computer engineering. He was the Founding Editor-In-Chief of the IEEE TRANSACTIONS ON SUSTAINABLE ENERGY and the IEEE ELECTRIFICATION MAGAZINE. He is the President-Elect of the IEEE Power and Energy Society for 2016 and 2017. In 2006, he served on the IEEE Board of Directors as the Vice President for publications. He served as the Chair of the US National Science Foundation Advisory Committee for International Science and Engineering from 2010 to 2013. He is a Distinguished Lecturer for the IEEE Power & Energy Society, and has lectured on smart grid, energy efficiency, renewable energy, demand response, distributed generation, and critical infrastructure protection topics in more than 30 countries on all six continents. He is an IEEE Millennium Medal winner.